Effects of Synoptic-Scale Control on Long-Term Declining Trends of Summer Fog Frequency over the Pacific Side of Hokkaido Island

SHIORI SUGIMOTO, TOMONORI SATO, AND KAZUKI NAKAMURA

Faculty of Environmental Earth Science, Hokkaido University, Sapporo, Japan

(Manuscript received 20 July 2012, in final form 30 April 2013)

ABSTRACT

In this study, long-term visibility data for the Pacific Ocean side of Hokkaido Island, northeast Japan, are investigated to clarify the relationship between interannual variation in summer fog frequency (FF) and large-scale circulation patterns. At Kushiro, a significant FF decrease is found during 1931–2010 even without the influence of the observatory's relocation after 2000. In particular, since the late 1970s, a linear declining trend has accelerated, as evidenced by an increased number of years with very low FF in July and August. To clarify the climatological factor causing the summer FF declining trend at Kushiro, atmospheric vertical conditions in the planetary boundary layer and large-scale circulation are examined during 1989–2009 and 1958–2002, respectively, using available datasets. Composite analyses that are based on radiosonde observations reveal that the shallow fog layer is covered with a strong inversion layer during fog days whereas the inversion layer is absent during nonfog days. Composite circulation anomalies for the low-FF years at Kushiro show an intensified Okhotsk high (OH) pressure feature and southward shrinking of the North Pacific high (NPH) in July, in addition to the eastward displacement or shrinking of the NPH in August. These anomalous synoptic circulation patterns cause weakening in the southerly–southeasterly wind, which reduces sea-fog advection toward Kushiro and prevents the formation of stable stratification over the sea-fog layer. The authors suggest that the interannual variation in summer FF with the recent accelerated decline at Kushiro is primarily controlled by changes in the synoptic circulation associated with the OH and NPH development.

1. Introduction

Marine stratiform clouds and fogs, which are typically distributed over subtropical and midlatitude oceans (Warren et al. 1988; Houze 1993; Klein and Hartmann 1993; Norris and Leovy 1994; Lewis et al. 2004), are crucial for the energy balance of the earth (e.g., Hartmann et al. 1992). Long-term variability of low-level clouds with and without fog events has been investigated by a considerable number of studies to understand its role in global climatic change (e.g., Norris et al. 1998; Norris 1999; Clement et al. 2009; Lauer et al. 2010).

During summer, sea fog is frequently observed over cold ocean currents in the Northern Hemisphere, particularly over the Oyashio in the North Pacific Ocean and the Labrador Current in the North Atlantic Ocean (Lewis et al. 2004; Eastman et al. 2013). This sea fog is attributed to the cooling of the abundant warm, moist air transported from the south by the oceanic midlatitude subtropical anticyclone (Lewis et al. 2004; Gultepe et al. 2007). Over the western North Pacific, sea-fog formation has been intensively investigated in the offshore areas around northeastern Japan (Sea Fog Research Team 1985; Sawai 1988; Klein and Hartmann 1993; Norris 1998; Tanimoto et al. 2009; Tokinaga et al. 2009). Data from the Japan Meteorological Agency (JMA) observatories indicate that the sea fog often migrates into the coastal areas of Hokkaido Island in northern Japan (Fig. 1). Moreover, JMA observation data from 1951 to 1980 indicate that fog days account for approximately 50% of summer days in southeastern Hokkaido Island (Sawai 1988). Such high fog frequency causes low visibility, which leads to frequent traffic accidents (Uyeda and Yagi 1982). In addition, agriculture is significantly affected by the fog-affected local climate through factors such as low sunshine duration, low temperatures, and high humidity (Yakuwa 1953). Therefore, long-term fog variability is an important topic for the region's residents. The JMA's historical fog-frequency datasets over land could be useful for the understanding of

Corresponding author address: Shiori Sugimoto, Hokkaido University, North 10 East 5, Kita-Ku, Sapporo 060-0810, Japan.
E-mail: shioris@ees.hokudai.ac.jp

DOI: 10.1175/JAMC-D-12-0192.1

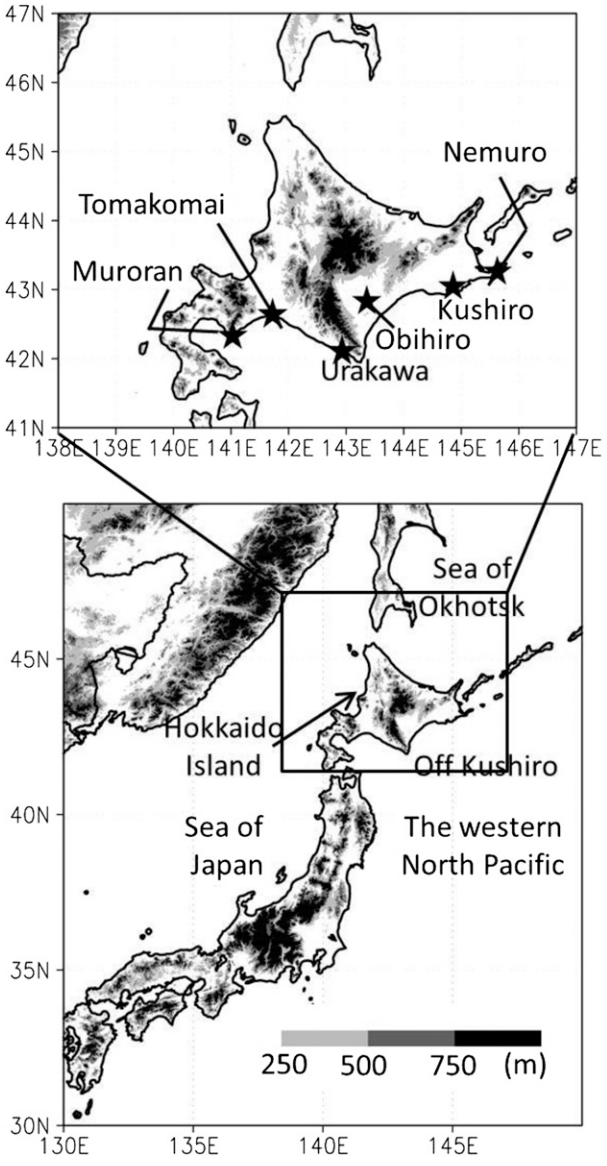

FIG. 1. Topography of the study area. Stars indicate locations of meteorological observatories used in this study.

fog-frequency variation and could be a surrogate index for climatological atmospheric and oceanic changes near the western North Pacific as well as changes in the local meteorological environment.

In general, sea fog is strongly affected by the atmospheric structure in the planetary boundary layer up to approximately 1000 m. Therefore, a dataset with high vertical resolution is essential for discussing the atmospheric vertical structure that causes long-term sea-fog variation. Although radiosonde observation is advantageous for its high vertical resolution, few observation sites are available. In contrast, reanalysis data generally represent synoptic-scale atmospheric environment over several decades; the vertical resolution is coarse, however. It is expected that the combination of these two datasets can be sufficient for investigating the roles of large-scale environmental changes in long-term sea-fog variation in the near surface layer. In particular, a temperature difference between the atmosphere and ocean has been often adopted for estimating sea-fog generation over the ocean (Pilié et al. 1979; Dorman et al. 1998; Cho et al. 2000; Koracin et al. 2001; Lewis et al. 2003). Reanalysis-based temperature difference is easily calculated and suggests a possibility for generating sea fog over the ocean; this value is insufficient for discussing fog frequency observed in coastal land areas, however. To understand long-term variation in fog frequency over land, the large-scale circulation patterns must be considered because fog frequency is affected by the sea-fog advection from the ocean to land. Low-level air temperature inversion is an additional important and considerable issue for fog duration and continuous fog advection because stable stratification prevents fog diffusion and dissipation associated with vertical mixing (Haraoka et al. 1995).

In this study, we examine the interannual variation in fog frequency in northeastern Japan by analyzing 80 years of JMA observation data. In addition, the physical mechanism that controls the variation in fog frequency is investigated by using reanalysis data and upper-air observations. The detailed description of datasets is addressed in section 2. In section 3, we explain interannual and long-term variations in summertime fog frequency. Atmospheric vertical profiles obtained during fog days (FDs) and nonfog days (NFDs) are shown in section 4. Section 5 addresses the relationship between interannual variation in fog frequency and synoptic-scale circulation. The mechanism of interannual and long-term trends in fog frequency is discussed in section 6.

2. Data description

This study used the surface meteorological observation data obtained near the Pacific side of Hokkaido Island to investigate the fog-frequency variation and a possible influence of the local elements. In addition, the radiosonde data observed in the southeastern area of Hokkaido were used for diagnosis of the vertical profile during the fog event. Atmospheric and oceanic reanalysis data were applied to verify the large-scale control on fog-frequency variation.

a. Surface meteorological data

This study examined data from six JMA observatories on the Pacific side of Hokkaido Island: Muroran, Tomakomai, Urakawa, Obihiro, Kushiro, and Nemuro (Fig. 1). Obihiro observatory is located inland

TABLE 1. Altitude above mean sea level, wind measurement height from the ground, and floor numbers at the Muroran (Muror), Tomakomai (Tomak), Urakawa (Uraka), Obihiro (Obihi), Nemuro (Nemur), and Kushiro (Kushi) observatories. Floor number is given for an indication of visual observation height. Distance to the closest windward coast from each observatory and prevailing wind direction for fog days are also shown with direction to the coast. For Nemuro, with a peninsular location, two sets of values for distance/direction are given because the prevailing wind direction differs from the direction of the closest windward coast. For Kushiro, the first and second values represent before and after observatory relocation, respectively.

	Muror	Tomak	Uraka	Obihi	Nemur (peninsular)	Kushi
Alt (m)	40	6	37	45	25	32; 5
Floor no.	3	Unknown	2	2	4	3; 9
Wind monitor H (m)	18.2	20.1	17.9	11.3	29.2	22.0; 65.9
Distance (km)/direction to the coast	3.0/E	0.9/SE	0.4/SE	50/ESE	0.9/N; 3.0/S	1.3/S; 2.0/S
Prevailing wind direction	ENE	SE–SSE	ESE–SE	ENE–ESE	SE–S	SSE–S

approximately 50 km from the southeast coast (Table 1), and the other five observatories are located within 3 km of the coastline and parallel to the prevailing wind. The altitude of each observatory is lower than 45 m above mean sea level, indicating that the observatories are situated in a typical fog-layer thickness of several hundred meters, as reported in earlier observations (Yanagisawa et al. 1986; Uematsu et al. 2005). Further information for each observatory is summarized in Table 1.

To investigate the long-term variation in fog frequency, we used monthly fog-frequency (FF) data recorded at the six JMA observatories before 2010. The JMA has compiled monthly FF reports at Nemuro, Kushiro, Obihiro, Urakawa, and Muroran since 1931 and at Tomakomai since 1943. The FF, defined as the number of days with fog occurrences regardless of formation time or duration, has been reported for each month of each year. We did not exclude rainy days from the monthly FF statistics. The fog occurrence is assigned when visibility becomes less than 1000 m; therefore, fog observation has been conducted irregularly. Fog and low-level clouds are distinguished by whether the touchdown of the cloud base is recognized. Visibility is monitored through visual observation at the observatory's rooftop. Therefore, the monitoring altitude slightly differs depending on the observatories; altitude is shown in Table 1 as an indication of observation height. The Tomakomai and Urakawa observatories introduced automated visibility sensors in October of 2004 and 2009, respectively. Also note that in October of 2000 the meteorological observatory at Kushiro was redeployed from the previous site (42.977°N, 144.387°E) to the current location (42.985°N, 144.377°E), which is farther from the southern coast. As a result, the new observatory is still located in the coastal region but has been moved to approximately 700 m downwind of the previous location relative to the prevailing wind direction for the fog days, which is southerly.

In addition to FF, other meteorological variables, such as air temperature, relative humidity, and precipitation during 1931–2010 and wind speed during 1951–2010, were analyzed. The frequency of rainy days, defined as the number of days with precipitation exceeding 0.5 mm per day, was also examined for 1931–2010. At the Kushiro observatory, the wind measurement height was changed to reflect the observatory's relocation in October of 2000. Therefore, the wind speed after 2000 was corrected by the following equation:

$$U_b = U_a \left[\frac{\ln(z_b/z_0)}{\ln(z_a/z_0)} \right],$$

where U_a is the original wind speed ($\mathrm{m\,s^{-1}}$), U_b is the corrected wind speed ($\mathrm{m\,s^{-1}}$), $z_a = 22.0$ (m) is the altitude of the measurement until 2000, $z_b = 65.9$ (m) is the altitude of measurement after 2000, and $z_0 = 0.1$ (m) is the roughness length (Kondo 2000).

To examine the effects of sea-fog advection onto land, the frequency of wind direction was analyzed for FDs and for NFDs at six observatories during 1989–2010. The temporal interval of the wind direction data is 1 h except for those in 1989, which contain 3-h interval data; these values were combined for simplicity.

b. Radiosonde data

In section 4, we examine the vertical atmospheric profiles for FDs and NFDs. As previously mentioned, because the vertical resolution of the reanalysis data is too coarse for the purpose of this study, we analyzed the radiosonde data observed at Nemuro during 1989–2009 (Fig. 1). The Nemuro station is the only available observation site in central and eastern part of the southern Hokkaido Island. The radiosonde was launched two times per day at 0900 and 2100 LT (UTC + 9 h). Each sounding dataset was interpolated vertically at 10-m intervals. The observations at 0900 and 2100 LT were averaged to create the daily mean vertical profile because the fog usually occurs during the midnight–early morning hours between two radiosonde observations (not shown). The available lowest levels of the

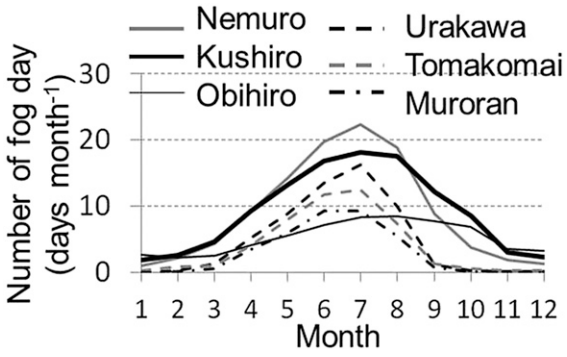

FIG. 2. Seasonal variation in FF averaged over 1931–2010 at Nemuro, Kushiro, Obihiro, Urakawa, and Muroran observatories and over 1943–2010 at Tomakomai observatory.

sounding were 50 m for temperature and humidity and 200 m for wind speed/direction.

c. Reanalysis data

The synoptic-scale control of the FF is discussed in section 5 by using the 40-yr European Centre for Medium-Range Weather Forecasts (ECMWF) Re-Analysis (ERA-40; Uppala et al. 2005) on a 2.5° × 2.5° grid. For sea surface temperature (SST), the National Oceanic and Atmospheric Administration (NOAA) Extended Reconstructed SST dataset, version 3 (NOAA-ERSST V3; Smith et al. 2008), on a 2° × 2° grid was used. Both atmospheric and oceanic analyses were conducted using monthly mean datasets obtained for 1958–2002. As discussed in section 6, the ERA-Interim reanalysis data (Dee et al. 2011) were used for additional atmospheric reanalysis data filling after 2002.

3. Seasonal and long-term variation in fog frequency

a. Seasonal variation in fog frequency

The mean seasonal variations in FF at the six observatories are shown in Fig. 2. The FF reduced to a minimum of a few days per month during winter and began to increase in spring at all observatories. At Obihiro, FF remained high throughout summer and autumn, with no significant peaks. In contrast, maximum FF occurred in June or July at the five coastal observatories of Nemuro, Kushiro, Urakawa, Tomakomai, and Muroran, which indicates that the fog types differ between coastal and inland regions. The summer FF peak in coastal regions is likely attributed to sea-fog advection. FF at the five coastal observatories gradually decreased from August to November. The decrease in FF at Kushiro was slower than that at the other observatories. The maximum FF was relatively higher at the eastern observatories of

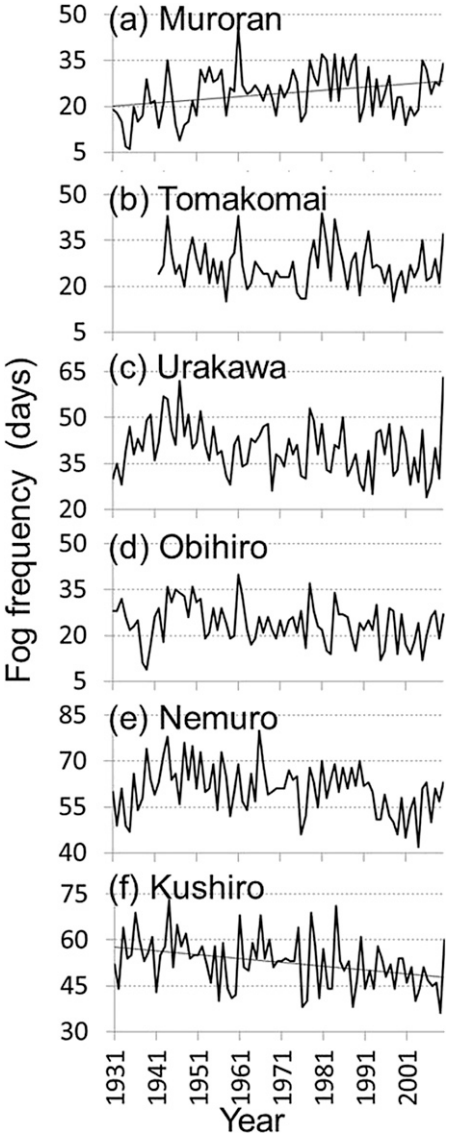

FIG. 3. Interannual variation in summer (JJA) FF (days) at (a) Muroran, (b) Tomakomai, (c) Urakawa, (d) Obihiro, (e) Nemuro, and (f) Kushiro from 1931 to 2010. In (a) and (f) the linear trend on the basis of the 99% confidence level is indicated by thin straight lines.

Nemuro and Kushiro than at the western observatories of Urakawa, Tomakomai, and Muroran. The seasonal-variation results indicate that the fog occurrence was most frequent during summer [June–August (JJA)], except at the inland observatory at Obihiro. That is, summer is an important season for considering long-term FF variation associated with sea-fog advection at the Pacific-side observatories at Hokkaido Island. Furthermore, the formation mechanism of fog during the cold season, which is mostly related to radiative cooling and local land surface processes, is likely to differ from that in the warm season. Therefore, long-term FF

TABLE 2. Gradient and p value of the linear trend in summer FF variation at each observatory. In the Kushi column, the left and right values are calculated for 1931–2010 and 1931–2000 (i.e., before the observatory relocation), respectively. The single and double asterisks indicate that the trend is statistically significant at the 95% and 99% confidence levels, respectively. See Table 1 for site abbreviations.

	Muror	Tomak	Uraka	Obihi	Nemur	Kushi
Gradient [days (10 yr)$^{-1}$]	1.05**	−0.27	−0.84*	−0.71*	−0.87*	−1.24**; −1.06*
p value	0.005	0.516	0.04	0.027	0.023	0.002; 0.033

variation during summer is the main focus in the following sections.

b. Long-term trend in summer fog frequency

Figure 3 shows interannual variation in the JJA total FF recorded at the six observatories over 1931–2010, with linear trends verified by the least squares method (Metcalfe 1994). The gradient of long-term summer FF trends and the significance p values are summarized in Table 2. Among the six observation sites, the only the Kushiro observatory experienced a significant declining trend with a 99% confidence level (Fig. 3f and Table 2), which appeared to have a weak influence on the multidecadal-scale variation that was evident at other observatories located near the coast (Figs. 3a,b,e; see the appendix for a detailed description). Moreover, the gradient of the FF declining trend at Kushiro is larger than that at other sites (Table 2). This unique 80-yr FF decline with the large gradient at Kushiro distinctly differs from FF variation at other sites; therefore it is worthy to examine in this study.

The FF decrease at Kushiro has accelerated in two periods: before 1960 and after the late 1970s. The FF decline in the former period is similar to that at other observation sites: Urakawa (Fig. 3c), Obihiro (Fig. 3d), and Nemuro (Fig. 3e), whereas the FF decrease in the latter period is a unique feature at Kushiro that was not evident at other coastal observatories. The declining trend in summer FF at Kushiro remained significant, with a 95% confidence level, even if the postrelocation data were excluded (Table 2). This evidence suggests that particular consideration must be given to the reason for the summer FF interannual variation with the long-term declining trend at Kushiro, in addition to the influence of the relocation.

c. Fog frequency in summer and local meteorological conditions at Kushiro

To reveal the month responsible for the summer FF decline at Kushiro, the interannual variation during 1931–2010 was analyzed for each month of JJA (Figs. 4a–c). The trend of FF decline before the site relocation was statistically significant only in August, with a 99% confidence level (Fig. 4c). Similar to the JJA total variation, the FF variation in August is characterized by two periods: from 1945 to the early 1960s and after the late 1970s. During the latter period, years with low FF, which are marked by spike-shaped signals in Fig. 4c, tended to occur more frequently. Circles in Figs. 4b and 4c indicate the years that correspond to the lowest 10% of FF for each month, referred to as low-FF years (Table 3). The number of low-FF years rapidly increased after the 1970s in August. A recent increase in the low-FF years was also observed in July, although the FF decline was not statistically significant (Fig. 4b). We suggest that July and August are the key months for the recent FF decline at

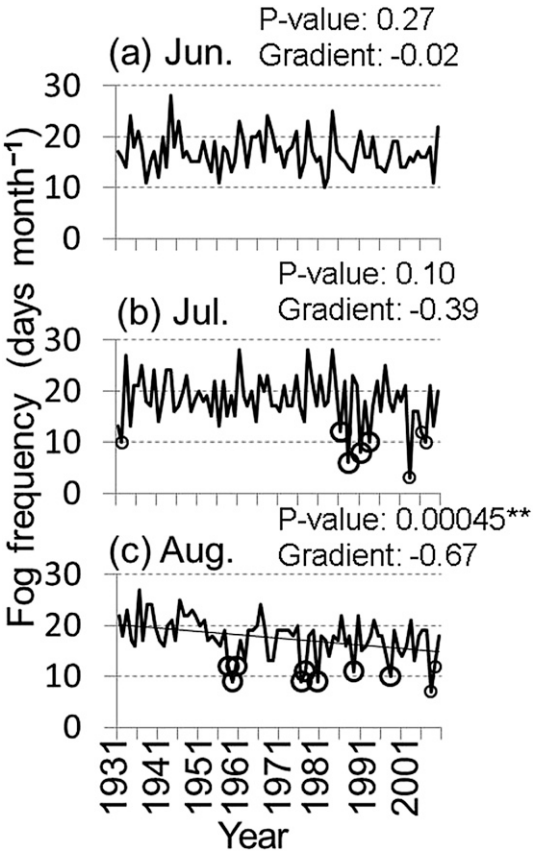

FIG. 4. Interannual variations in monthly FF (days month^{-1}) at Kushiro during summer in (a) June, (b) July, and (c) August. The linear trend indicates statistically significant trends with a 99% confidence level. Open circles in (b) and (c) represent low-FF years. Years marked by large circles were used for the composite analysis in section 5. The P value and gradient (days per decade) of linear trend in summer FF variation were added in each panel.

TABLE 3. Low-FF years for July and August.

Jul	1986, 1988, 1991, 1993
Aug	1958, 1959, 1960, 1976, 1977, 1980, 1989, 1998

Kushiro, particularly after the 1970s. Note that the low-FF years in July are not identical to those in August (Table 3). Furthermore, FFs in July and August have no meaningful correlation, which suggests that the factors controlling the monthly FF in July differ from those in August.

A long-term variation in air temperature, humidity, and wind speed is possibly controlling fog generation, dissipation, and diffusion. In addition, long-term decline of FF may be attributed to the change in rainfall amount and frequency of rainy days. To investigate the relationship between the FF decline and local atmospheric environmental changes in July and August, the interannual variations in relative humidity, air temperature, wind speed, monthly precipitation amount, and rainy-day frequency observed at Kushiro were examined before the site relocation. Relative humidity decreased significantly in both July and August, and its interannual variation was consistent with that in FF (Figs. 5a,b). In contrast, a warming trend in air temperature was not clear during 1931–2010 in July and August. The wind speed and monthly precipitation (precipitation not shown) do not show significant long-term decrease or increase trends in either month. The correlation between monthly FF and monthly rainy-day frequency was not statistically significant in summer months during 1931–2010 (not shown), indicating that fog is clearly distinguished from precipitation by the JMA's visual monitoring. These evidences indicate that, before the Kushiro observatory relocation, the FF linear trend is independent of variation in local atmospheric factors such as temperature, wind speed, and precipitation.

For sea-fog advection, wind direction is also an important atmospheric factor. Figure 6 shows the wind direction frequency and mean wind speed calculated for FDs (720 days) and NFDs (644 days) at Kushiro in July and August during 1989–2010. For the FDs at Kushiro, wind direction from the south-southeast and south (from the ocean to land) was dominant, with mean wind speeds of 3.1 and 3.3 $m\,s^{-1}$, respectively. The frequency of the northerly wind (west-northwest–east-northeast; from the land to sea) accounted for only 24% of the FDs, which suggests that the land breeze did not prevail during FDs and that many of the fog events in Kushiro are likely to occur under the condition of southerly wind intrusion. For NFDs, the prevailing wind direction shifted to north-northeast and northeast, with mean wind speeds of 4.2 and 3.6 $m\,s^{-1}$, respectively, which differs from that for FDs.

Surface observations suggest that the prevailing wind direction is an important physical factor for the change in interannual variation in summer FF, which is expected to affect recent increases in low-FF years in July and August. In the following section, the vertical atmospheric structure over eastern Hokkaido Island is analyzed and is compared between FDs and NFDs.

4. Vertical atmospheric structure for fog and nonfog days

Previous studies observed the vertical structures of sea fog at the coastal area of northeastern Japan. For

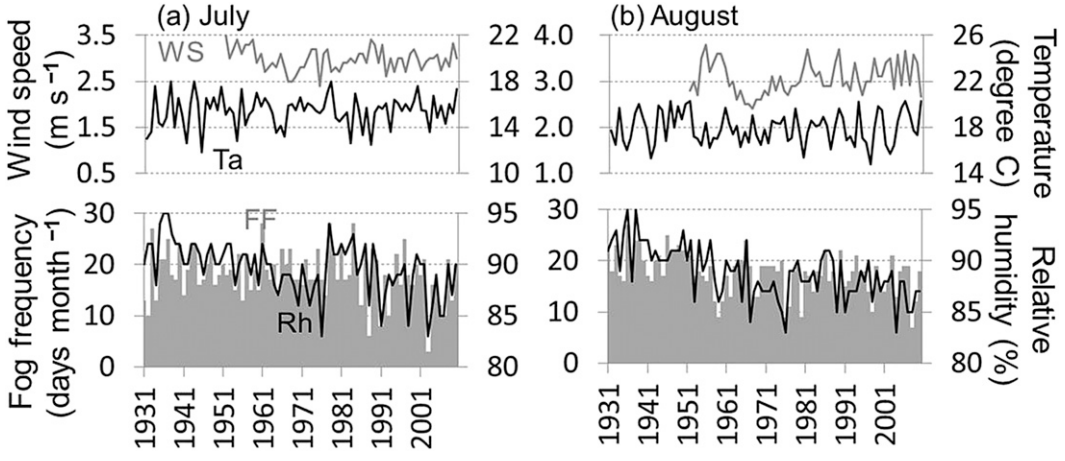

FIG. 5. Interannual variation in monthly averaged air temperature (Ta; black line and right-axis scale in the top panels), wind speed (WS; gray line and left-axis scale in the top panels), and relative humidity (Rh; black line and right-axis scale in the bottom panels) at Kushiro in (a) July and (b) August. Interannual variation in monthly FF is also indicated in the bottom panels by a gray bar (left-axis scale).

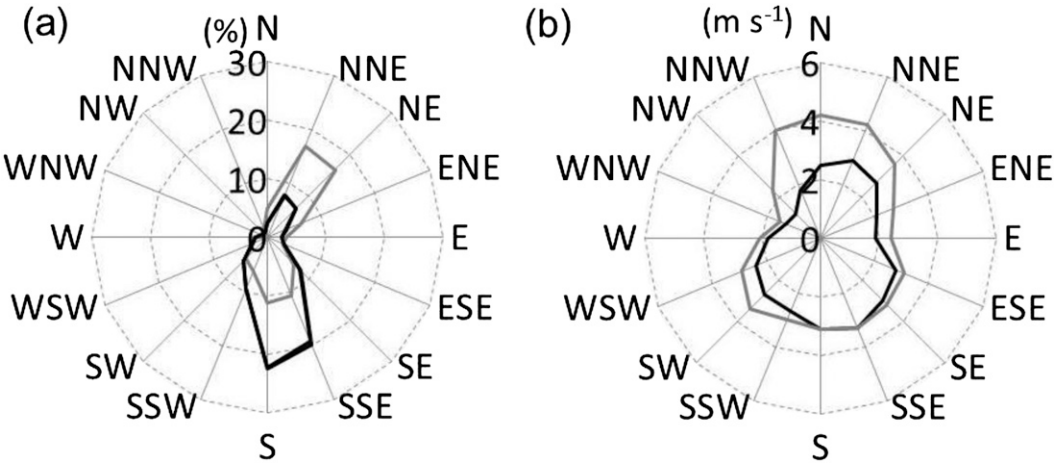

FIG. 6. (a) Frequency of wind direction and (b) mean wind speed for each wind direction at Kushiro for FDs (black curve) and NFDs (gray curve).

example, a sea-fog layer developed that was up to several hundred meters high (Yanagisawa et al. 1986; Uematsu et al. 2005) and was capped at the top by a strong inversion layer (Haraoka et al. 1995). The atmospheric vertical structure during NFDs has not yet been adequately understood, however. To clarify the atmospheric conditions responsible for low FF in July and August, we compared the vertical structure in the planetary boundary layer between FDs and NFDs. In this section, FDs and NFDs were classified using datasets of daily fog-occurrence information from Kushiro during July and August in 1989–2009. The analysis period for FDs and NFDs at Kushiro differs from that shown in section 3 because of the radiosonde data availability. By using the daily radiosonde observation data from Nemuro (section 2), a composite of daily mean profiles was computed for 677 FDs and 625 NFDs. Although the lowest level of the radiosonde sounding at Nemuro (approximately 50 m above mean sea level) was higher than the level of visibility monitoring at Kushiro (approximately a few tens of meters above mean sea level), this altitude difference had little impact on the comparison of the planetary boundary layer conditions between FDs and NFDs because the fog layer was expected to reach a few hundred meters above mean sea level, as previously described.

The composite vertical profiles of temperature, equivalent potential temperature, relative humidity, specific humidity, and wind in the lower troposphere for FDs are presented in Fig. 7a. In the lowest layer (below 200 m; shading in Fig. 7a), the temperature decreased with height and relative humidity was higher than 90%, which indicates fog occurrence in the shallow moist mixing layer. The mean height of the moist mixing layer was slightly shallower than that shown in the case studies in which the fog layer reached several hundred meters above sea level (Yanagisawa et al. 1986; Uematsu et al. 2005). Above the mixing layer, a temperature inversion was present up to approximately 400 m above sea level. Between 80 and 400 m above sea level, specific humidity reached its maximum level ($11.2\,g\,kg^{-1}$) and the equivalent potential temperature increased with height at a rate of $2.1\,K\,(100\,m)^{-1}$, thus demonstrating that the strongly stable inversion layer consists of moist air. The conditions of high specific humidity and convectively stable stratification in the inversion layer are important for preserving fog droplets from dissipation by mechanical and convective mixing at the top of the shallow mixing layer (Haraoka et al. 1995). Wind direction rotated clockwise with height from south-southwesterly to west-southwesterly, which suggests that the advection of moist and warm air from the south is expected to play a positive role in the formation of the shallow fog layer and the moist inversion layer.

The vertical structure for NFDs is shown in Fig. 7b. The temperature inversion was remarkably weak in the lower troposphere. Moisture profiles showed lower relative humidity at less than 88% and lower specific humidity at less than $10\,g\,kg^{-1}$ from the surface to 2000 m, which indicates that atmospheric conditions near the surface are drier for NFDs than for FDs. Above a level of 120 m, the equivalent potential temperature increased with height at a lower rate of approximately $0.6\,K\,(100\,m)^{-1}$ up to 1400 m. A weak easterly–northerly wind direction was dominant below 1000 m, and northwesterly winds of less than $3.0\,m\,s^{-1}$ were dominant between 1000 and 2000 m. The northerly and northwesterly wind caused a dry and cool intrusion, which led to unsuitable

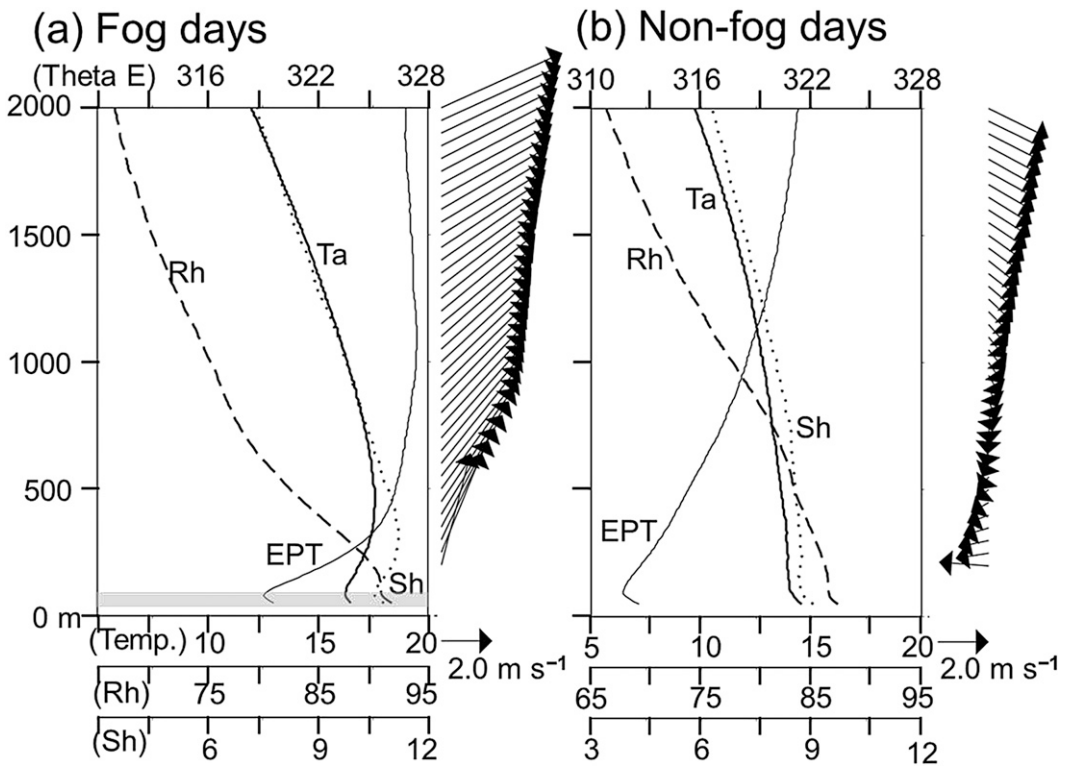

FIG. 7. Composite of vertical profile of temperature [Ta (°C); thick black line], relative humidity [Rh (%); dashed line], specific humidity [Sh ($g\,kg^{-1}$); dotted line], equivalent potential temperature [EPT (K); gray thick line], and horizontal wind ($m\,s^{-1}$; arrows) at Nemuro for (a) FDs and (b) NFDs. Gray shading in (a) indicates a shallow moist layer.

conditions for fog-layer formation around the eastern region of Hokkaido Island.

In FD cases, the southerly component of wind was dominant near the surface layer, which was similar to the surface observation at Kushiro, shown in Fig. 6a. A moist inversion layer with stable stratification developed over the shallow fog layer. In contrast, NFD cases are characterized by an environment that is cooler and drier than that for FD, with prevailing northerly–northwesterly winds originating from a cold oceanic air mass around the Sea of Okhotsk. These results indicate that the difference in the vertical atmospheric structure between FD and NFD cases is strongly related to the prevailing wind direction in the lower troposphere. Furthermore, vertical profiles of wind for FDs and NFDs are in good agreement with the observed evidence in Kushiro shown in section 3, which suggests that the wind direction is controlled by large-scale circulation covering the southeastern region of Hokkaido Island. In the following section, synoptic-scale atmospheric environment, which decides the dominant wind direction, is examined by using reanalysis data to clarify the cause of the long-term interannual variation in FF with a decline after the late 1970s at Kushiro during summer.

5. Synoptic-scale circulation controlling the fog-frequency variability

As mentioned in section 3, summer FF decline accelerates at Kushiro during 1931–2010 as evidenced by recent increases in the low-FF years. The radiosonde and in situ observations indicate that lower-tropospheric wind direction is distinctly different between FDs and NFDs. This evidence suggests that interannual variation and long-term linear declining trend in the FF at Kushiro are likely to be attributable to advection of sea fog and warm, moist air. In this section, the available reanalysis data are analyzed for 1958–2002 to understand the synoptic-scale circulation in the lower troposphere that causes a low-FF year during summer. Because the low-FF years in July and August are not identical (Table 3), the controlling mechanism for the low-FF years may also differ between July and August; hence, these months are investigated separately. The low-FF years shown in Table 3 and Fig. 4 were selected for the composite analysis of circulation patterns in low-FF years.

We hereinafter focus on synoptic-scale circulation patterns at 1000 and 925 hPa for several reasons. Near-surface

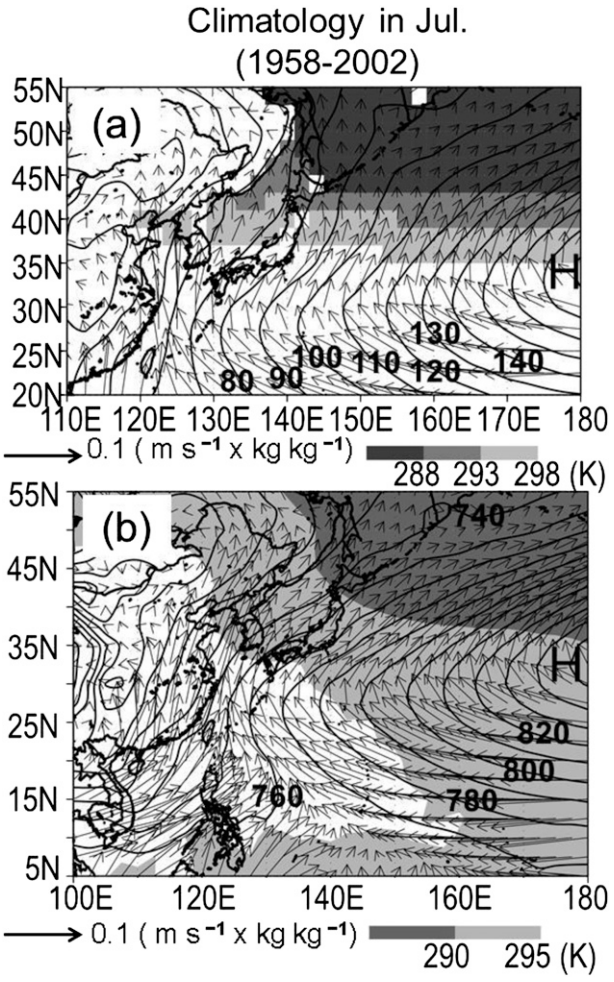

FIG. 8. Spatial distribution of the climatological geopotential height (contour; gpm) and moisture flux ($q\mathbf{V}$; $\mathrm{m\,s^{-1}\,kg\,kg^{-1}}$) at (a) 1000 and (b) 925 hPa in July. Shadings in (a) and (b) represent SST (K) and air temperature at 925 hPa, respectively. A larger domain (5°–55°N, 100°E–180°) is used in (b).

level (1000 hPa) provides the direction of sea-fog advection and associated pressure gradient because the sea-fog advection toward Kushiro occurs in a shallow layer of only a few hundred meters above the sea surface. The 925-hPa level corresponds to the atmosphere above the fog layer. The warm advection in this layer creates stability at the top of the fog layer. Moreover, moisture advection at 925 hPa is necessary for the high humidity that maintains fog droplets in the upper portion of the sea-fog layer.

a. July

Figure 8a shows the climatological mean of SST, geopotential height, and water vapor flux at 1000 hPa in July. The western edge of the North Pacific high (NPH) pressure system reached 130°E along a ridge near 27.5°N. Moist southerly wind penetrated into northeastern Japan along the NPH anticyclonic circulation. Offshore near Kushiro, the SST was cooler than the Sea of Japan at the same latitude because of the presence of the cold Oyashio from the north. The moisture advection over the Oyashio from the south is consistent with the observation results of sea fog generated over the western North Pacific (e.g., Tanimoto et al. 2009; Tokinaga et al. 2009). These atmospheric and oceanic conditions are suitable for sea-fog generation, which is attributed to the cooling of the abundant warm and moist air transported from the south by the anticyclonic circulation, as well as the Labrador Current (Gultepe et al. 2007). The northward wind direction also contributes to northward sea-fog advection from offshore to onshore around Kushiro. The wind direction over Hokkaido Island shifted slightly from the south at 1000 hPa to the southwest at 925 hPa (Fig. 8b). The southwesterly wind at 925 hPa transported warm air from the subtropical region to northeastern Japan. The difference in synoptic-scale circulation between 1000 and 925 hPa was such that, at 925 hPa, the monsoon westerlies and the easterly-wind branch of the anticyclonic circulation of the NPH converged near 17.5°N, 120°E. The convergence of the two moist flows appeared to enhance the moisture transport to northeastern Japan because specific humidity increased near the convergence area (not shown). This circulation pattern at 925 hPa was favorable for the formation of the moist inversion layer above the sea-fog layer, which causes consecutive fog occurrence as mentioned in section 4.

The composites of anomalous circulations at 1000 and 925 hPa for low-FF years are shown in Figs. 9a and 9b, respectively. At both pressure levels, the geopotential height in low-FF years shows a high pressure anomaly over the Sea of Okhotsk and a low pressure anomaly centered on 38°N, 165°E. The positive anomaly of the geopotential height near the Sea of Okhotsk indicates stronger Okhotsk high (OH) activity in the low-FF years relative to the climatological value. The negative anomaly near the western North Pacific indicates suppression of the northward extension of the NPH in July during the low-FF years. In association with the geopotential height anomaly, the moisture flux at 1000 hPa shows anomalous southwestward moisture transport over northern Japan, indicating that northward sea-fog advection rarely occurred in the low-FF years. The mean air temperature at 925 hPa in the low-FF years was lower than climatological values by more than 1.5 K at 35°–45°N, 130°–160°E near Kushiro, suggesting insufficient development of the moist inversion layer above the sea fog. In summary, stronger OH and weaker northward extension of the NPH diminished the southerly–southwesterly

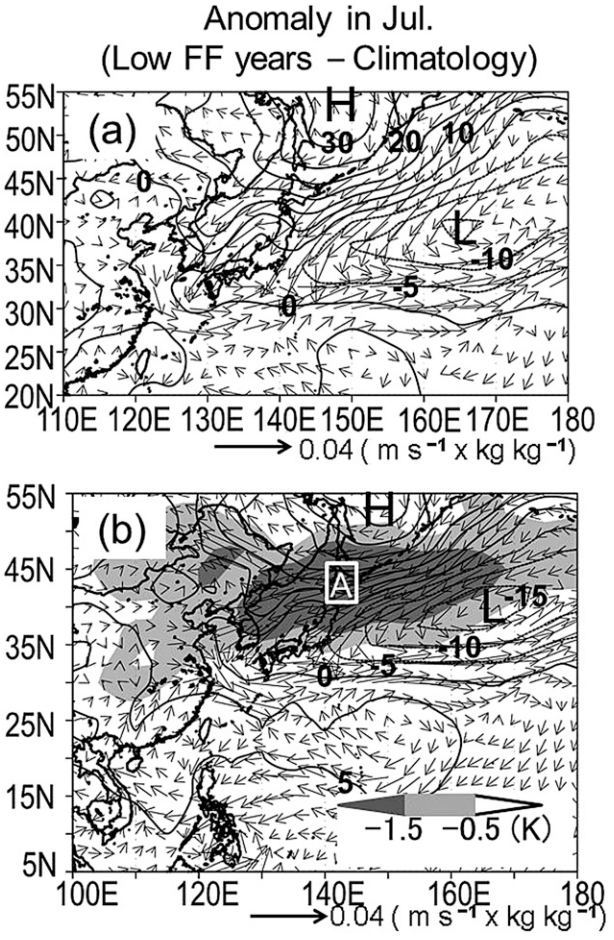

FIG. 9. (a) Low-FF years and climatological differences in geopotential height (gpm) and $q\mathbf{V}$ ($\mathrm{m\,s^{-1}\,kg\,kg^{-1}}$) at 1000 hPa in July. (b) As in (a), but at 925 hPa; a larger domain (5°–55°N, 100°E –180°) is used in (b). Light shading and dark shading in (b) indicate temperature anomalies greater than −0.5 and −1.5 K, respectively. The open square in (b) shows domain A, as described in section 5.

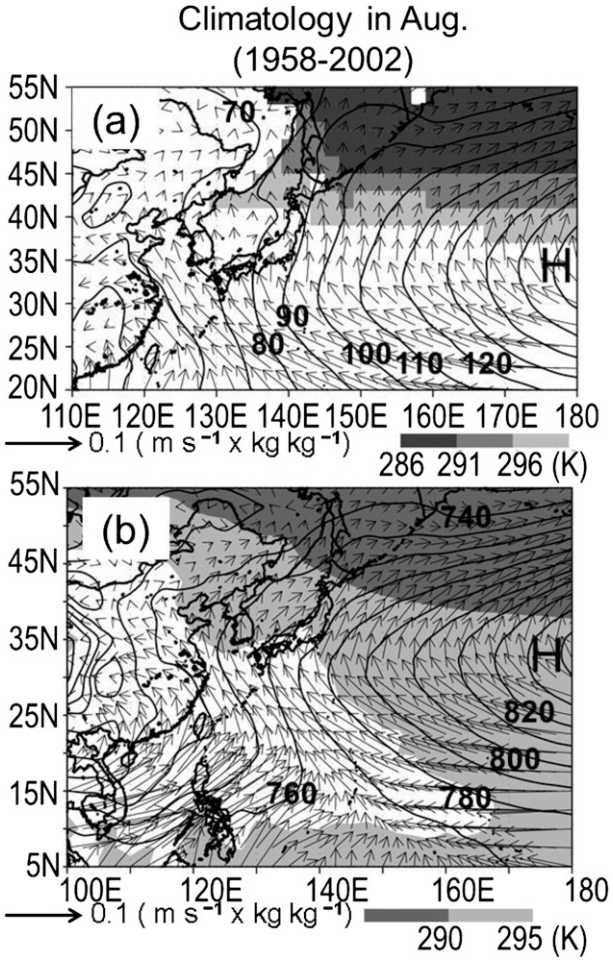

FIG. 10. As in Fig. 8, but for August.

wind around northeastern Japan in July of low-FF years. The weakening of the southerly wind at 1000 hPa reduced the sea-fog transport toward Kushiro, and the cold anomaly at 925 hPa weakened the inversion layer, resulting in shorter fog duration near Kushiro.

b. August

August climatological patterns (Figs. 10a,b) revealed that the NPH receded slightly eastward and extended more northward at 1000 and 925 hPa near Japan than that observed in July. Therefore, the eastern part of Hokkaido Island was covered by the NPH. The northward extension of the NPH was also observed in the composite of low-FF years (not shown). Although the distribution of the NPH in August differed slightly from that in July, the southerly (southwesterly) wind toward Kushiro was still dominant at 1000 (925) hPa. The cool SST caused by the cold Oyashio off Kushiro was present in August as well as in July (Fig. 10a). The northward moisture transport at 1000 hPa established suitable conditions for fog generation off Kushiro in the region of cool SST and for sea-fog migration to the coastal area on the Pacific side of Hokkaido Island. At 925 hPa (Fig. 10b), the southwesterly wind over Japan transported a warm and moist air mass from the subtropical region, which was also observed in the July climatological values.

The anomaly of the geopotential height in the low-FF years in August differed from that in July. The high pressure anomaly over the Sea of Okhotsk, which was observed in July, was not evident in August (Figs. 11a,b), suggesting that the formation mechanism of low-FF conditions differed between the two months. This speculation is also consistent with the fact that the low-FF years differed between July and August (Table 3).

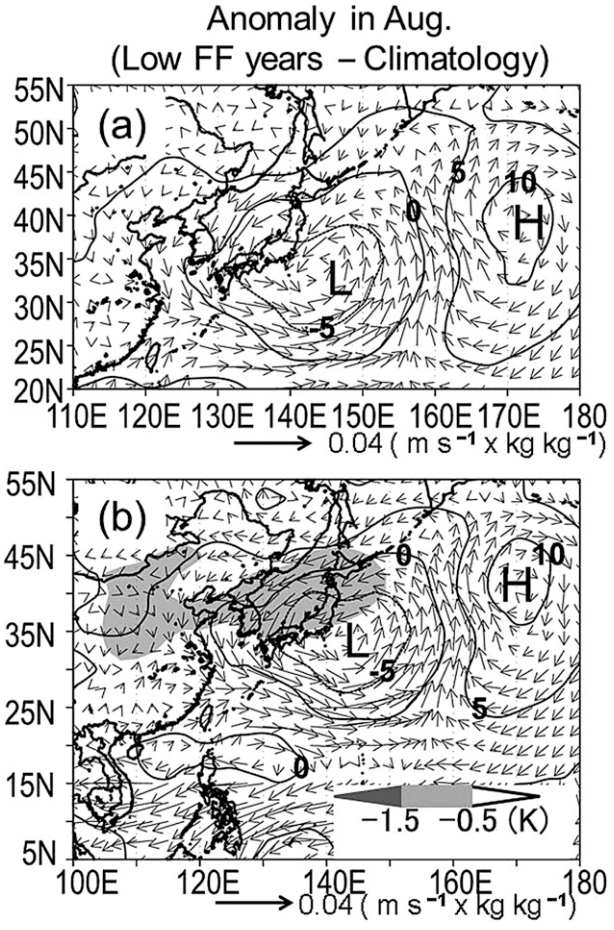

FIG. 11. As in Fig. 9, but for August.

In August, the geopotential height showed zonal high and low anomalies characterized by a low pressure anomaly centered near 33°N, 145°E and a high pressure anomaly centered near 40°N, 173°E at both 1000 and 925 hPa. This distribution of the geopotential height anomaly indicates a weakened westward extension of the NPH in the low-FF years. The cyclonic anomaly at the western part of the NPH suppressed northeastward moisture transport at both levels and formed cool atmospheric conditions near northern Japan at 925 hPa. These atmospheric conditions at 1000 and 925 hPa are similar to those observed in July of low-FF years. At 925 hPa, an anomalous westward flow was detected near the Philippines, south of 15°N between 100° and 130°E (Fig. 11b), which was not significant in July. This result indicates that the monsoon westerly was weaker in August of the low-FF years than that shown in climatology. The weaker monsoon westerly caused a weaker convergence along the NPH edge, which is likely to reduce moisture transport toward northeastern Japan.

Composite analysis revealed that, in August, eastward displacement of the NPH was prominent in the low-FF years, which weakened moisture and heat transport toward northeastern Japan along the NPH edge. The weakening of monsoon westerlies at 925 hPa was an additional factor in the reduction of moisture convergence in the subtropics, which is associated with a lower moisture supply than that observed during the normal years. These features of synoptic-scale circulation patterns in low-FF years differ significantly from the vertical atmospheric structure required for sea-fog advection.

For both July and August, the weakening of warm advection in a low-FF year causes more obvious temperature decrease in the near-surface atmospheric layer than that at the sea surface (not shown). As a result, a physical parameter ΔT, which is calculated by surface air temperature minus SST, becomes smaller in a low-FF year relative to the climatological value. For example, in July, ΔT averaged over the offshore of Kushiro (40°–44°N, 144°–154°E) had a climatological value of +0.9 K and was +0.2 K in the low-FF years; the corresponding values were +0.5 and +0.4 K in August, respectively. This result suggests an inactive sea-fog generation in the low-FF year, which is consistent with the FF variation at Kushiro.

Composite analysis for July and August suggests that the frequency of the low-FF years at Kushiro after 1958 is primarily characterized by weakened moisture and heat supply from the south in association with the NPH shape. In the following section, interannual variation in FF is examined on the basis of synoptic-scale atmospheric variables in association with warm advection and moisture advection.

6. Relationship between interannual fog-frequency variation and synoptic-scale environment

The composite analysis in the previous section revealed circulation anomalies in July and August that caused low-FF years. To understand the relationship between synoptic-scale circulation change and interannual FF variation with accelerated FF decline after the late 1970s (Fig. 3f), this section presents the statistical analysis. Two indices were analyzed using the monthly mean reanalysis data for 1958–2002: SW925, the southwest component of wind vector averaged over Hokkaido (40°–45°N, 140°–145°E; domain A in Fig. 9b) and the OH index (OHI; Tachibana et al. 2004), defined as geopotential height at 850 hPa averaged over 55°–57.5°N and 147.5°–157.5°E. SW925 represents the northward fog-advection ability and the intensity of heat and moisture supply above the fog layer, both of which are important for stable stratification and a humid environment above the fog layer. OHI represents the intensity of the OH, which brings the

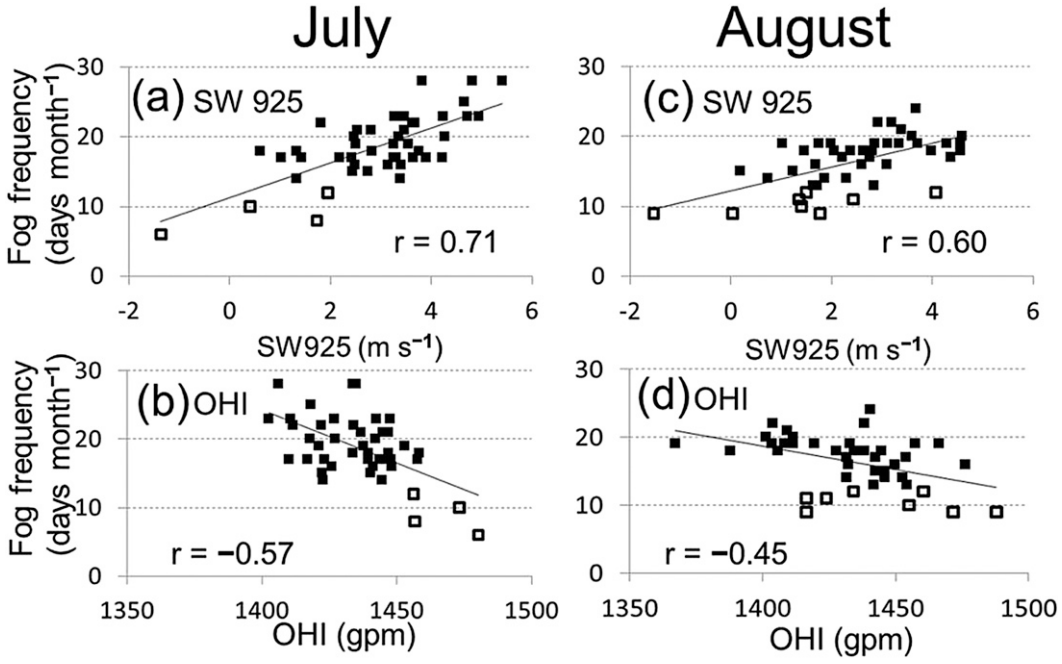

FIG. 12. Scatter diagram for FF at Kushiro and synoptic-scale indices for (left) July and (right) August for (a),(c) SW925 and (b),(d) OHI. Open squares indicate low-FF years.

northeasterly wind near Kushiro. Figure 12 shows the relationship between the circulation indices and FF at Kushiro. For July (Figs. 12a,b), statistically significant correlations were detected for SW925 (correlation coefficient $r = 0.71$) and OHI ($r = -0.57$), with a 99% confidence level. In August (Figs. 12c,d), correlations were also significant for SW925 ($r = 0.60$) and OHI ($r = -0.45$); the correlation coefficients were smaller than those in July, however.

Because SW925 outperformed OHI for both months and was a crucial factor for FF variation, we compared the interannual variation in July–August mean SW925 and July–August total FF at Kushiro (Fig. 13). ERA-40 ended in 2002; therefore, ERA-Interim was overlaid for 1979–2010. This index is not sensitive to the choice of the reanalysis dataset because SW925 from the two reanalysis datasets is very similar during 1979–2002. The SW925 index follows the interannual variation in FF. Moreover, this index successfully predicted the timing of low-FF years. The interannual variation after 1958 with declining trend for SW925 during 1978–2000 was consistent with that in FF, which strongly suggests that the declining trend in FF after the late 1970s until the observatory's relocation in 2000 at Kushiro is attributed to the change in large-scale circulation rather than to local factors. The SW925 index did not follow the interannual variation in FF after 2000, however. It is highly probable that the local environment in the vicinity of the observatory changed because of relocation in 2000, which caused the relationship between SW925 and FF to deteriorate. Although the new observatory's altitude is approximately 27 m lower than that of the previous site, this altitude difference has little impact on FF variation because both new and previous observatory sites are included in the sea-fog layer of a few hundred meters thickness according to the vertical profile shown in Fig. 7a. A plausible explanation for the FF decrease after the

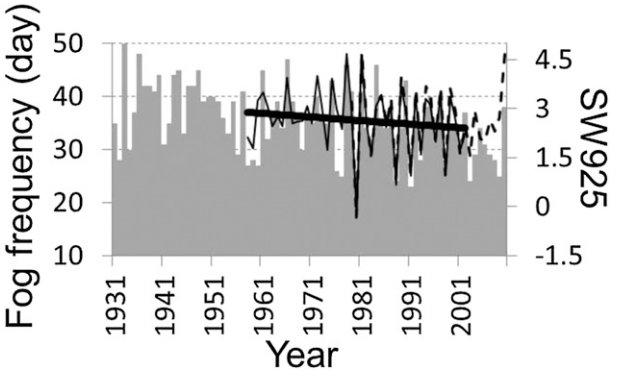

FIG. 13. Interannual variation in July–August total FF at Kushiro (gray bar) and July–August mean SW925 index (thin solid black line) as determined by ERA-40. The black dashed line indicates the SW925 index calculated by using ERA-Interim data from 1979 to 2010. The linear-regression line for the SW925 index as determined using ERA-40 is indicated by the thick solid black line.

relocation is that the distance of sea-fog advection passing over the urban area from upstream of the southern coast was increased, which consequently hastened fog dissipation. As a result, the SW925–FF relationship was broken after 2000; since then, FF variation can scarcely be explained by SW925. Figure 13 suggests that SW925 was a useful surrogate index of FF at Kushiro during mid- to late summer and is able to capture FF interannual variation.

The comparison of interannual variations between the surrogate index and the observed FF indicates that the relocation of the Kushiro observatory significantly affected low FF in the last decade, in addition to large-scale circulation changes. The reanalysis data have an advantage of validating large-scale changes, whereas the difference between the reanalysis and local observation provides information on the influence of local environment changes that are not considered by the reanalysis (e.g., Kalnay and Cai 2003). Further studies are needed to evaluate the local effects on the recent FF variation at Kushiro by use of comprehensive observations and by conducting numerical experiments that use a mesoscale model.

7. Discussion

a. The relationship between large-scale circulation change and the long-term FF variation at other observatories

We examined the long-term FF decline at Kushiro, which was strongly controlled by synoptic-scale circulation in association with the NPH expansion. If the large-scale circulation controlled the interannual FF variation with the recent accelerated decline at Kushiro since 1978, it is probable that other observatories experienced similar FF variations. The relationship between the FF variation at other observation sites and SW925, defined in section 6, is examined using ERA-40 datasets for 1958–2002. The correlation coefficients between SW925 and the July–August total FF are 0.38 (Muroran), 0.40 (Tomakomai), 0.53 (Urakawa), 0.39 (Obihiro), and 0.26 (Nemuro), which are obviously lower than that for Kushiro ($r = 0.71$). Furthermore, the correlations at Muroran, Obihiro, and Nemuro are not statistically significant. This result indicates that the large-scale circulation pattern change associated with the NPH distribution is insufficient for explaining the interannual FF variations at the other five observatories, which differ from the FF variation at Kushiro.

We should consider reasons why the long-term FF variations at the other five sites are not affected by large-scale circulation associated with the NPH distribution. Figure 14 shows the wind direction frequency

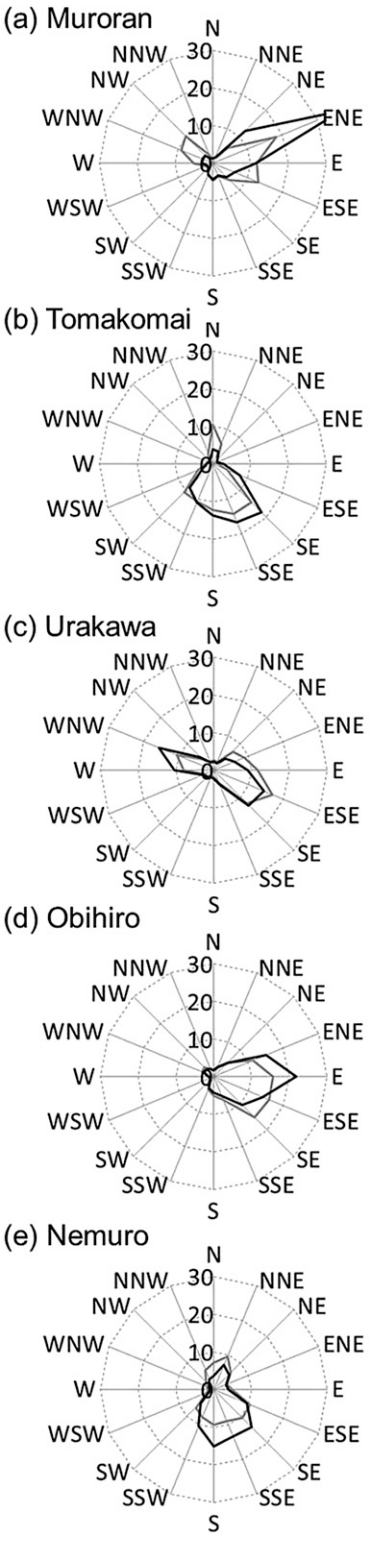

FIG. 14. As in Fig. 6a, but for (a) Muroran, (b) Tomakomai, (c) Urakawa, (d) Obihiro, and (e) Nemuro.

for FDs and NFDs at the five observatories during 1989–2010, except for Kushiro. Dominant wind directions for FDs were from southeast to south at Nemuro, from the east at Obihiro, from east-southeast and southeast at Urakawa, from southeast and south-southeast at Tomakomai, and from east-northeast at Muroran. These results indicate that the fog events at the four observatories—that is, Muroran (Fig. 14a), Urakawa (Fig. 14c), Obihiro (Fig. 14d), and Nemuro (Fig. 14e)—tended to occur under easterly and southeasterly winds, suggesting a different large-scale condition from that at Kushiro, where the fog event favors southerly wind. At Tomakomai (Fig. 14b), southeasterly wind dominates for both FDs and NFDs, indicating that the efficiency of sea-fog advection by large-scale circulation has little impact on the FF variation. That is, a suitable wind direction for fog occurrence and the influence of the synoptic-scale circulation distinctly differ between Kushiro and the other five observatories because of the complex coastline geometry in the southern part of Hokkaido Island. Therefore, only at Kushiro does the intensity of southerly wind in association with the NPH distribution affect the significant declining trend in summer FF.

Indeed, the southerly wind did not correspond to the winds from the ocean for the five observatories if the local shoreline curve is considered. We suggest that the relationship between dominant wind direction and distance from the closest shoreline is crucial for large-scale sea-fog advection. For example, the FF significantly decreased after the relocation of Kushiro observatory just 700 m northward from the previous site as discussed in section 6. The easterly wind component was frequently observed around the southern part of Hokkaido Island, including the region over the ocean, under the southward expansion of OH centered east of Hokkaido (Takai et al. 2006; Shimada et al. 2010), which suggests that the OH behavior is likely to have a stronger influence on the sea-fog advection toward the other observatories.

b. Possibility of the NPH distribution change in the past and future climate

We revealed that the position of the NPH is crucial for interannual variation in the summer FF. Many previous studies have focused on the mechanism of the NPH variability in summer (e.g., Nitta 1987; Enomoto et al. 2003; Xie et al. 2009; Kosaka and Nakamura 2006, 2010). For example, the NPH in August becomes weak over Japan when the eastward wave propagation along the subtropical jet, known as the Silk Road pattern (Enomoto et al. 2003), is inactive. Enomoto (2004) reported that the Silk Road pattern was not prominent in 1952, 1970, 1975, 1979, and 1996. This kind of NPH behavior did not appear in the low-FF years (Table 3), however. Instead, the northeastward Rossby-wave propagation emanating from the convective activity over the subtropical western Pacific controls the horizontal extension of the NPH, which is known as the Pacific–Japan pattern (Nitta 1987; Kosaka and Nakamura 2010). The convective activity over the subtropical western Pacific is strongly affected by El Niño–Southern Oscillation (ENSO). Xie et al. (2009) indicated that the summer convective activity over the subtropical western Pacific is suppressed following an El Niño peak because of an active baroclinic Kelvin wave forced by the warm tropical Indian Ocean. These variations in tropical forcing may have affected the recent increase in the low-FF years since the 1970s. In fact, Wu and Wang (2002) and Wang et al. (2008) indicated that the coupling between ENSO and the western North Pacific summer climate has strengthened since the late 1970s. They further demonstrated that the anticyclonic anomaly becomes dominant over the western North Pacific and that the cyclonic anomaly appears over central Japan during the decaying phase of El Niño. Their reported anomalous circulation pattern is similar to the composite for low-FF years examined in this study (Figs. 9 and 11), which suggests that the recent decline in FF at Kushiro could be explained as a remote effect of ENSO. Note that several low-FF years shown in Table 3 and Fig. 4 occurred after El Niño winters (i.e., 1958, 1977, 1988, 1998, and 2003) or after winter seasons with an El Niño–like SST anomaly (i.e., 1980 and 2007). Although a more comprehensive analysis is necessary, it is suggested that low-FF years tend to occur during the decaying phase of El Niño through the modification of NPH development.

General circulation models used to perform future projections of the global climate indicate a weakening of the NPH's northward extension during summer and that of its anticyclonic circulation as a result of increasing greenhouse gases in association with suppressed convective activity over the tropical western Pacific (Kimoto 2005; Kitoh and Uchiyama 2006; Kosaka and Nakamura 2011). These findings are also consistent with the recent increase in the low-FF years. Further studies are needed, particularly for the monitoring and modeling of low-level clouds over the ocean.

This study investigated the role of synoptic-scale circulation in the declining trend of FF at Kushiro in summer. The interannual variation in FF at some observatories exhibited similarities, as mentioned in section 3 and the appendix; long-term trends differed significantly among the observatories, however. These results could be attributed to various historical backgrounds of local

environments, such as the influence of the Kushiro observatory relocation, and different sensitivities to the synoptic-scale circulation change. It is important to maintain long-term monitoring of local surface meteorological conditions to diagnose local environmental change and synoptic-scale climate variability.

8. Summary

The long-term FF trend at the Pacific side of Hokkaido Island, northern Japan, was investigated by analyzing 80 years of visibility data recorded during 1931–2010. At Kushiro, summer FF has significantly decreased since 1931, even if the observatory relocation is not considered. In particular, the decline of summer FF has accelerated since the late 1970s as evidenced by the fact that the number of low-FF years has been increasing in both July and August. In situ observation data indicate that southerly wind occurs frequently on FDs at Kushiro.

The radiosonde observation data were analyzed to understand the vertical atmospheric structure during fog events. A shallow fog layer was covered by a strong moist inversion layer during FDs. In contrast, during NFDs, an inversion layer was not evident in the radiosonde observations. The vertical profile of the wind direction strongly suggests that a northerly–northeasterly wind plays a key role in preventing the development of the inversion layer during NFDs. A composite analysis of synoptic-scale circulation for the low-FF years in July and August was conducted to identify the possible influence of large-scale circulation on the interannual variation in summer FF with recent accelerated decline at Kushiro after the late 1970s. We revealed that either NPH or OH variability, or both, controls lower tropospheric circulation to affect FF. In July, the intrusion of warm and moist air masses from subtropical regions was weaker in the low-FF years because of a weaker northward extension of the NPH and development of OH. In August, the intensity of the northward heat and moisture transport near the western edge of the NPH at 925 hPa was affected by the westward extension of the NPH, which controlled the northward moisture supply from the monsoon westerly.

As per the regression analysis, the SW925 index showed the highest correlation with interannual variation in FF in both July and August. The interannual variation after 1958 and the decreasing trend during 1978–2000 in SW925 are consistent with the FF decline in both months. Therefore, we conclude that the cause of the long-term declining trend in summer FF at Kushiro is attributed to the weakening of SW925, which particularly increased the frequency of the low-FF years after the late 1970s.

The relocation of the Kushiro observatory is an additional factor for the rapid decrease in FF in the past decade. Influences of ENSO and global warming are also possible. The NPH development is likely to be affected by tropical SSTs, and it is suggested that the low-FF years tend to occur during decaying phases of El Niño.

Acknowledgments. This work was partially supported by the Research Program on Climate Change Adaptation (RECCA) and GRENE Arctic Climate Change Research Project of the Ministry of Education, Culture, Sports, Science and Technology (MEXT), the Environment Research and Technology Development Fund [S-8-1(2)] of the Ministry of the Environment, Japan, and the Grant-in-Aid for Scientific Research on Innovative Areas (25106701) funded by JSPS. Fog-frequency data and radiosonde observation data were provided by JMA. ERA-40 and ERA-Interim data were provided by the ECMWF. SST data of NOAA-ERSST V3 were provided by the National Climatic Data Center. We are grateful to Ms. Akiko Shouji, Mr. Atsushi Wajima, Mr. Satoshi Yamanaka, Mr. Yuji Yamada, Mr. Kazuhiro Tanabe, and Mr. Satoshi Sugawara at Japan Meteorological Agency for their helpful advice.

APPENDIX

Interannual Variation in Summer FF at Five Observation Sites

Long-term interannual variations in JJA total FF at Muroran, Tomakomai, Urakawa, Obihiro, and Nemuro are examined for 1931–2010 and are described here. At the Muroran observatory, the increasing trend in summer FF was significant with a 99% confidence level during 1931–2010 because of a remarkable upward trend until 1960 (Fig. 3a and Table 2). This increasing trend is a unique feature that does not appear at other observatories. After 1960, the multidecadal-scale variation became more dominant at Muroran and Tomakomai in comparison with the linear trend (Figs. 3a,b). At both observatories, high FF was observed in the 1980s, and FF decreased during 1960–80 and after the 1990s. In addition, interannual variations in summer FF at Muroran and Tomakomai are very similar and have statistically significant correlation of $r = 0.58$, which suggests that FF variation at these two sites was under the strong control of similar synoptic-scale forcing. As described in section 7, easterly wind is dominant at Muroran in FDs, which distinctly differs from the prevailing wind direction at Kushiro in FDs. For Tomakomai, southerly wind is frequently observed in both cases of FDs and NFDs,

suggesting that wind direction strongly depends on the topography. This evidence at Tomakomai indicates that an impact of large-scale circulation change of FF variation is possibly smaller than that at other observatories. Thus, the factor controlling FF variation is different between Kushiro and two western observatories; therefore, long-term declining trend in FF variation is not significant at Muroran and Tomakomai.

At Urakawa observatory, the multidecadal-scale variation was very weak in summer FF variation (Fig. 3c). An abrupt FF increase in 2010 may be attributed to the introduction of an automated visibility sensor, which needs validation after data accumulation. A significant decreasing trend, with a 95% confidence level, that was detected during 1930–2010 (Table 2) was caused by an FF decrease during 1945–60 (Fig. 3c). A similar FF decrease appeared at Obihiro observatory (Fig. 3d). The summer FF variation at Obihiro fluctuated between 12 and 30 days after 1960, except for several spike-shaped peaks appearing in 1961, 1978, and 1984. A declining trend in summer FF was significant at Nemuro observatories with a 95% confidence level (Fig. 3e and Table 2). A multidecadal-scale variation, which is similar to that in the western area, was obvious in the interannual variation in summer FF at Nemuro. In particular, the significant low-FF period after 1990 contributes to make a large gradient in the long-term summer FF decline trend.

A significant trend is not confirmed in air temperature and wind speed at the five observatories, except for wind speed at Tomakomai. Relative humidity significantly increases at only Muroran and decreases at the other four observation sites, which is consistent with FF variation at each site. A correlation between FF and rainy-day frequency is also not significant at the five sites. These evidences indicate that an influence of local atmospheric environment is small on the long-term trend at the five observatories, which is similar to the result at Kushiro.

REFERENCES

Cho, Y.-K., M.-O. Kim, and B.-C. Kim, 2000: Sea fog around the Korean Peninsula. *J. Appl. Meteor.,* **39,** 2473–2479.

Clement, C. A., R. Burgman, and J. R. Norris, 2009: Observational and model evidence for positive low-level cloud feedback. *Science,* **325,** 460–464.

Dee, D. P., and Coauthors, 2011: The ERA-Interim reanalysis: Configuration and performance of the data assimilation system. *Quart. J. Roy. Meteor. Soc.,* **137,** 553–597.

Dorman, C. E., L. Armi, J. M. Bane, and D. P. Rogers, 1998: Sea surface mixed layer during the 10–11 June 1994 California coastally trapped event. *Mon. Wea. Rev.,* **126,** 600–619.

Eastman, R., S. G. Warren, and C. J. Hahn, 2013: Climatic atlas of clouds over land and ocean. [Available online at http://www.atmos.washington.edu/CloudMap/.]

Enomoto, T., 2004: Interannual variability of the Bonin high associated with the propagation of Rossby waves along the Asian jet. *J. Meteor. Soc. Japan,* **82,** 1019–1034.

——, B. J. Hoskins, and Y. Matsuda, 2003: The formation mechanism of the Bonin high in August. *Quart. J. Roy. Meteor. Soc.,* **129,** 157–178.

Gultepe, I., and Coauthors, 2007: Fog research: A review of past achievements and future perspective. *Pure Appl. Geophys.,* **164,** 1121–1159.

Haraoka, H., K. Tomine, T. Kawabata, K. Miyamoto, and K. Fukawatase, 1995: Some aspects on temperature, humidity and wind profiles in sea fog at Misawa city (in Japanese). *Tenki,* **42,** 369–379.

Hartmann, L. D., M. E. Ockert-Bell, and M. L. Michelsen, 1992: The effect of cloud type on Earth's energy balance: Global analysis. *J. Climate,* **5,** 1281–1304.

Houze, R. A., Jr., 1993: *Cloud Dynamics.* Academic Press, 573 pp.

Kalnay, E., and M. Cai, 2003: Impact of urbanization and land-use change on climate. *Nature,* **423,** 528–531.

Kimoto, M., 2005: Simulated change of the East Asian circulation under global warming scenario. *Geophys. Res. Lett.,* **32,** L16701, doi:10.1029/2005GL023383.

Kitoh, A., and T. Uchiyama, 2006: Changes in onset and withdrawal of the East Asian summer rainy season by multi-model global warming experiments. *J. Meteor. Soc. Japan,* **84,** 247–258.

Klein, A. S., and D. L. Hartmann, 1993: The seasonal cycle of low stratiform clouds. *J. Climate,* **6,** 1587–1606.

Kondo, J., 2000: *Atmospheric Science near the Ground Surface.* University of Tokyo Press, 324 pp.

Koracin, D., J. Lewis, W. T. Thompson, C. E. Dorman, and J. A. Businger, 2001: Transition of stratus into fog along the California coast: Observations and modeling. *J. Atmos. Sci.,* **58,** 1714–1731.

Kosaka, Y., and H. Nakamura, 2006: Structure and dynamics of the summertime Pacific–Japan teleconnection pattern. *Quart. J. Roy. Meteor. Soc.,* **132,** 2009–2030.

——, and ——, 2010: Mechanisms of meridional teleconnection observed between a summer monsoon system and a subtropical anticyclone. Part I: The Pacific–Japan pattern. *J. Climate,* **23,** 5085–5108.

——, and ——, 2011: Dominant mode of climate variability, intermodal diversity, and projected future change over the summertime western North Pacific simulated in the CMIP3 models. *J. Climate,* **24,** 3935–3955.

Lauer, A., K. Hamilton, Y. Wang, V. T. J. Phillips, and R. Bennartz, 2010: The impact of global warming on marine boundary layer clouds over the eastern Pacific—A regional model study. *J. Climate,* **23,** 5844–5863.

Lewis, J., D. Koracin, R. Rabin, and J. Businger, 2003: Sea fog off the California coast: Viewed in the context of transient weather systems. *J. Geophys. Res.,* **108,** 4457, doi:10.1029/2002JD002833.

——, ——, and K. T. Redmond, 2004: Sea fog research in the United Kingdom and United States. *Bull. Amer. Meteor. Soc.,* **85,** 395–408.

Metcalfe, A. V., 1994: *Statistics in Engineering: A Practical Approach.* Chapman and Hall, 446 pp.

Nitta, T., 1987: Convective activities in the tropical western Pacific and their impact on the Northern Hemisphere summer circulation. *J. Meteor. Soc. Japan,* **65,** 373–390.

Norris, R. J., 1998: Low cloud type over the ocean from surface observations. Part I: Relationship to surface meteorology and the vertical distribution of temperature and moisture. *J. Climate,* **11,** 369–382.

——, 1999: On trends and possible artifacts in global ocean cloud cover between 1952 and 1995. *J. Climate,* **12,** 1864–1870.

——, and C. B. Leovy, 1994: Interannual variability in stratiform cloudiness and sea surface temperature. *J. Climate,* **7,** 1915–1925.

——, Y. Zhang, and J. M. Wallace, 1998: Role of low clouds in summertime atmosphere–ocean interactions over the North Pacific. *J. Climate,* **11,** 2482–2490.

Pilié, R. J., J. Mack, C. W. Rogers, U. Katz, and W. C. Kocmond, 1979: The formation of marine fog and the development of fog-stratus systems along the California coast. *J. Appl. Meteor.,* **18,** 1275–1286.

Sawai, T., 1988: Sea fog in Kushiro District (in Japanese). *Tenki,* **35,** 555–566.

Sea Fog Research Team, 1985: Observations of sea fog in Kushiro District (in Japanese). *Tenki,* **32,** 41–52.

Shimada, T., M. Sawada, W. Sha, and H. Kawamura, 2010: Low-level easterly winds blowing through the Tsugaru Strait, Japan. Part I: Case study and statistical characteristics based on observations. *Mon. Wea. Rev.,* **138,** 3806–3821.

Smith, T. M., R. W. Reynolds, T. C. Peterson, and J. Lawrimore, 2008: Improvements to NOAA's historical merged land–ocean surface temperature analysis (1880–2006). *J. Climate,* **21,** 2283–2296.

Tachibana, Y., T. Iwamoto, M. Ogi, and Y. Watanabe, 2004: Abnormal meridional temperature gradient and its relation to the Okhotsk high. *J. Meteor. Soc. Japan,* **82,** 1399–1415.

Takai, H., H. Kawamura, and O. Isoguchi, 2006: Characteristics of the *Yamase* winds over oceans around Japan observed by the scatterometer-derived ocean surface vector winds. *J. Meteor. Soc. Japan,* **84,** 365–373.

Tanimoto, Y., S.-P. Xie, K. Kai, H. Okajima, H. Tokinaga, T. Murayama, M. Nonaka, and H. Nakamura, 2009: Observations of marine atmospheric boundary layer transitions across the summer Kuroshio Extension. *J. Climate,* **22,** 1360–1374.

Tokinaga, H., Y. Tanimoto, S.-P. Xie, T. Sampe, H. Tomita, and H. Ichikawa, 2009: Ocean frontal effects on the vertical development of clouds over the western North Pacific: In situ and satellite observations. *J. Climate,* **22,** 4241–4260.

Uematsu, A., H. Hashiguchi, M. Teshiba, H. Tanaka, K. Hirashima, and S. Fukao, 2005: Moving cellular structure of fog echoes obtained with a millimeter-wave scanning Doppler radar at Kushiro. *J. Appl. Meteor.,* **44,** 1260–1273.

Uppala, S. M., and Coauthors, 2005: The ERA-40 Re-Analysis. *Quart. J. Roy. Meteor. Soc.,* **131,** 2961–3012.

Uyeda, H., and T. Yagi 1982: Observation of sea fogs at Kushiro in eastern Hokkaido (in Japanese with English abstract). National Research Institute for Earth Science and Disaster Prevention Rep. 29, 69–85.

Wang, B., J. Yang, T. Zhou, and B. Wang, 2008: Interdecadal changes in the major modes of Asian-Australian monsoon variability: Strengthening relationship with ENSO since the late 1970s. *J. Climate,* **21,** 1771–1789.

Warren, S. G., C. J. Hahn, J. London, R. M. Chervin, and R. L. Jenne, 1988: Global distribution of total cloud cover and cloud type amounts over the ocean. National Center for Atmospheric Research Tech. Note NCAR/TN-317+STR, 43 pp + appendixes. [Available online at http://opensky.library.ucar.edu/collections/TECH-NOTE-000-000-000-467.]

Wu, R., and B. Wang, 2002: A contrast of the East Asian summer monsoon–ENSO relationship between 1962–77 and 1978–93. *J. Climate,* **15,** 3266–3279.

Xie, S.-P., K. Hu, J. Hafner, H. Tokinaga, Y. Du, G. Huang, and T. Sampe, 2009: Indian Ocean capacitor effect on Indo–western Pacific climate during the summer following El Niño. *J. Climate,* **22,** 730–747.

Yakuwa, R., 1953: Characteristics of climatology in Hokkaido and its problem for agriculture (in Japanese). *J. Agric. Meteor.,* **8,** 149–154.

Yanagisawa, Z., M. Ishihara, and T. Sawai, 1986: Observations of sea fog by 8.6 millimeter radar (in Japanese). *Tenki,* **33,** 603–612.